

Lecture Notes in Production Engineering

Bernd-Arno Behrens

Alexander Brosius

Wolfgang Hintze

Steffen Ihlenfeldt

Jens Peter Wulfsberg *Editors*

Production at the leading edge of technology

Proceedings of the 10th Congress
of the German Academic Association
for Production Technology (WGP),
Dresden, 23–24 September 2020

WGP
Wissenschaftliche
Gesellschaft für
Produktionstechnik

 Springer

Lecture Notes in Production Engineering

Lecture Notes in Production Engineering (LNPE) is a new book series that reports the latest research and developments in Production Engineering, comprising:

- Biomanufacturing
- Control and Management of Processes
- Cutting and Forming
- Design
- Life Cycle Engineering
- Machines and Systems
- Optimization
- Precision Engineering and Metrology
- Surfaces

LNPE publishes authored conference proceedings, contributed volumes and authored monographs that present cutting-edge research information as well as new perspectives on classical fields, while maintaining Springer's high standards of excellence. Also considered for publication are lecture notes and other related material of exceptionally high quality and interest. The subject matter should be original and timely, reporting the latest research and developments in all areas of production engineering. The target audience of LNPE consists of advanced level students, researchers, as well as industry professionals working at the forefront of their fields. Much like Springer's other Lecture Notes series, LNPE will be distributed through Springer's print and electronic publishing channels. To submit a proposal or request further information please contact Anthony Doyle, Publishing Editor (anthony.doyle@springer.com).

More information about this series at <http://www.springer.com/series/10642>

Bernd-Arno Behrens · Alexander Brosius
Wolfgang Hintze · Steffen Ihlenfeldt
Jens Peter Wulfsberg
Editors

Production at the leading edge of technology

Proceedings of the 10th Congress of the
German Academic Association for Production
Technology (WGP), Dresden, 23–24
September 2020

Editors

Bernd-Arno Behrens
Institute of Forming Technology
and Machines
Garbsen, Germany

Steffen Ihlenfeldt
Institute of Mechatronic Engineering
Dresden, Germany

Alexander Brosius
Institute of Manufacturing Science
and Engineering
Dresden, Germany

Jens Peter Wulfsberg
Laboratorium for Manufacturing
Technology
Hamburg, Germany

Wolfgang Hintze
Institute of Production Management
and Technology
Hamburg, Germany

ISSN 2194-0525 ISSN 2194-0533 (electronic)
Lecture Notes in Production Engineering
ISBN 978-3-662-62137-0 ISBN 978-3-662-62138-7 (eBook)
<https://doi.org/10.1007/978-3-662-62138-7>

© The Editor(s) (if applicable) and The Author(s), under exclusive license to Springer-Verlag GmbH, DE, part of Springer Nature 2021

This work is subject to copyright. All rights are solely and exclusively licensed by the Publisher, whether the whole or part of the material is concerned, specifically the rights of translation, reprinting, reuse of illustrations, recitation, broadcasting, reproduction on microfilms or in any other physical way, and transmission or information storage and retrieval, electronic adaptation, computer software, or by similar or dissimilar methodology now known or hereafter developed.

The use of general descriptive names, registered names, trademarks, service marks, etc. in this publication does not imply, even in the absence of a specific statement, that such names are exempt from the relevant protective laws and regulations and therefore free for general use.

The publisher, the authors and the editors are safe to assume that the advice and information in this book are believed to be true and accurate at the date of publication. Neither the publisher nor the authors or the editors give a warranty, expressed or implied, with respect to the material contained herein or for any errors or omissions that may have been made. The publisher remains neutral with regard to jurisdictional claims in published maps and institutional affiliations.

Editorial contact: Alexander Grün

This Springer imprint is published by the registered company Springer-Verlag GmbH, DE part of Springer Nature.

The registered company address is: Heidelberger Platz 3, 14197 Berlin, Germany

Preface



In 2020, the annual congress of the German Academic Association for Production Technology (WGP) will be held as a Webinar from September 23th to 24th under the slogan “Production at its limits – shaping change through innovation”. The WGP is hosting its annual congress for the 10th time in a row.

On behalf of the WGP, the organizing institutes are looking forward to exciting discussions with experts from research.

Production research permanently shifts the boundaries of what is feasible. Under the slogan “Production at its limits”, the contributions show production processes that advance into new areas in terms of methodology, use of resources or interdisciplinary.

But where does the search for new borders lead to? Which borders do we still have to cross, which ones do we prefer not to cross?

The focus of the congress is on production processes in border areas related to extreme velocity, size, accuracy, methodology, use of resources and interdisciplinarity. Challenges from the fields of forming machines and processes, cutting machines and processes, additive processes, automated assembly and robotics, machine learning and management sciences will be addressed.

The conference transcript summarizes the contributions from production science and industrial research. They provide the readership with an overview of current trends in production research and give an insight into ongoing research by the German Academic Association for Production Technology.

We wish all participants an interesting and inspiring WGP annual congress.

September 2020

Prof. B.-A. Behrens



Prof. A. Brosius



Prof. W. Hintze



Prof. S. Ihlenfeldt



Prof. J. P. Wulfsberg



Organization

Gottfried Wilhelm Leibniz Universität Hannover
Institut für Umformtechnik und Umformmaschinen
Prof. Dr.-Ing. Bernd-Arno Behrens
Norman Heimes, M. Sc.
Dipl.-Ing. Daniel Rosenbusch

Technische Universität Dresden
Institut für Fertigungstechnik
Prof. Dr.-Ing. Alexander Brosius
Dipl.-Ing. Sebastian Langula

Technische Universität Hamburg
Institut für Produktionsmanagement und -technik
Prof. Dr.-Ing. Wolfgang Hintze
Dr.-Ing. Carsten Möller

Technische Universität Dresden
Institut für Mechatronischen Maschinenbau
Prof. Dr.-Ing. Steffen Ihlenfeldt
Friederike Edner, M. A.

Helmut-Schmidt-Universität – Universität der Bundeswehr Hamburg
Laboratorium Fertigungstechnik
Prof. Dr.-Ing. Jens Peter Wulfsberg
Lennart Hildebrandt, M. Sc.

Contents

Forming Machine Tools and Manufacturing Processes	
Experimental Characterisation of Tool Hardness Evolution Under Consideration of Process Relevant Cyclic Thermal and Mechanical Loading During Industrial Forging.	3
F. Müller, I. Malik, H. Wester, and B.-A. Behrens	
Modelling of Hybrid Parts Made of Ti-6Al-4V Sheets and Additive Manufactured Structures.	13
J. Hafenecker, T. Papke, F. Huber, M. Schmidt, and M. Merklein	
Investigation of a Superimposed Oscillation Compression Process for the Production of a Bulk Component	23
D. Rosenbusch, P. Müller, S. Hübner, K. Brunotte, and B.-A. Behrens	
Towards an Adaptive Production Chain for Sustainable Sheet-Metal Blanked Components	34
P. Niemiets, T. Kaufmann, M. Unterberg, D. Trauth, and T. Bergs	
Investigation on Noise Reduction During Cutting of High-Strength Materials Based on Machine Acoustic Simulation.	45
D. Friesen, R. Krimm, S. Fries, K. Brunotte, and B.-A. Behrens	
Equal-Channel-Angular-Swaging for the Production of Medical Implants Made of Fine-Grained Titanium.	56
L. Kluy, F. Chi, and P. Groche	
Numerical Development of a Tooling System for the Co-extrusion of Asymmetric Compound Profiles on a Laboratory Scale.	66
N. Heimes, J. Uhe, S. E. Thüerer, H. Wester, H. J. Maier, C. Klose, and B.-A. Behrens	
Investigation of the Phase Transformation in Hot Stamping Processes with Regard to the Testing Facility	76
A. Horn, T. Hart-Rawung, J. Buhl, M. Bambach, and M. Merklein	

Simulation of an Electromagnetic Foil-Feeding Device	86
O. Commichau, A. Höber, B.-A. Behrens, and R. Krimm	
Extension of Process Limits with Bidirectional Deep Drawing	96
S. Kriechebauer, P. Müller, R. Mauermann, and W.-G. Drossel	
Further Development of a Hydraulically Operated Oscillation Device for Application to an Industrial Forming Process	105
P. Müller, D. Rosenbusch, N. Missal, H. Vogt, S. Hübner, and B.-A. Behrens	
Investigation of Clinched Joints – A Finite Element Simulation of a Non-destructive Approach	116
B. Sadeghian, C. Guillaume, R. Lafarge, and A. Brosius	
Experimental Process Design for Reclamation of Geared Components	125
P. Kuwert, T. Petersen, K. Brunotte, and B.-A. Behrens	
A New Approach for the Evaluation of Component and Joint Loads Based on Load Path Analysis	134
C. Steinfelder and A. Brosius	
Microstructure and Mechanical Properties of Thermomechanically Forged Tempering Steel 42CrMo4	142
J. Diefenbach, K. Brunotte, and B.-A. Behrens	
Dynamic Performance of Polymer-Steel-Hybrids Manufactured by Means of Process Integration	151
M. Demes, T. Ossowski, P. Kabala, S. Bienia, and K. Dröder	
Investigation of the Scaling of Friction Coefficients from the Nano to the Micro Level for Base Materials and Coatings	161
N. Heimes, F. Pape, D. Konopka, S. Schöler, K. Möhwald, G. Poll, and B.-A. Behrens	
Investigation of Parameters Influencing the Producibility of Anodes for Sodium-Ion Battery Cells	171
J. Hofmann, A.-K. Wurba, B. Bold, S. Maliha, P. Schollmeyer, J. Fleischer, J. Klemens, P. Scharfer, and W. Schabel	
Numerical Investigation of an Extruded Shaft for High Temperature Applications Manufactured by Tailored Forming	182
C. Büdenbender, I. Ross, H. Wester, A. Zaitsev, and B. A. Behrens	
Introduction of Composite Hot Extrusion with Tubular Reinforcements for Subsequent Cold Forging	193
P. Kotzyba, K. C. Grötzinger, O. Hering, M. Liewald, and A. E. Tekkaya	
Experimental Springback Validation of a Finite Element Model of Multi-stage Stator Bending	202
D. Wüterich, M. Liewald, and M. Kopp	

Cutting Machine Tools and Manufacturing Processes

Concept of a Mechatronic System for Targeted Drill Head Direction and Angular Alignment Control in BTA Deep Hole Drilling 215
 J. F. Gerken and D. Biermann

Influence of a Two-Cut-Strategy on Tool Wear in Gear Hobbing 225
 N. Troß, J. Brimmers, and T. Bergs

Application Potential of Thermoelectric Signals for Temperature Monitoring in Turning of Aluminum Alloys 235
 T. Junge, A. Nestler, and A. Schubert

Modeling of Contact Conditions and Local Load in Bevel Gear Grinding 246
 M. Solf, J. Brimmers, and T. Bergs

Design of Pulsed Electrochemical Machining Processes Based on Data Processing and Multiphysics Simulation 256
 I. Schaarschmidt, S. Loebel, P. Steinert, M. Zinecker, and A. Schubert

Functional PVD Hard Coatings for High Temperature Cutting Processes 266
 N. Stachowski, N. C. Kruppe, T. Brögelmann, and K. Bobzin

Wear Behaviour of PCBN, PCD, Binderless PCBN and Cemented Carbide Cutting Inserts When Machining Ti-6Al-4V in an Oxygen-Free Atmosphere 275
 F. Schaper, B. Denkena, M.-A. Dittrich, A. Krödel, J. Matthies, and S. Worpenberg

Influence of Nozzle Position during Cryogenic Milling of Ti-6Al-4V 284
 K. Gutzeit, H. Hotz, B. Kirsch, and J. C. Aurich

Lifespan Investigations of Linear Profiled Rail Guides at Pitch and Yaw Moments 294
 S. Ihlenfeldt, J. Müller, and D. Staroszyk

Towards the Prediction of Compliance Influences on Shape Deviations in Internal Traverse Grinding 304
 N. Schmidt, T. Tsagkir Dereli, T. Furlan, R. Holtermann, D. Biermann, and A. Menzel

Numerical Modelling of the Aeroacoustic and Flow Behaviour of Chip Fans 315
 C. Menze, C. Zizelmann, M. Schneider, K. Güzel, and H.-C. Möhring

Estimation of the Influence of Volumetric Correction Approaches on the Thermo-Elastic Correction Accuracy 324
 X. Thiem, B. Kauschinger, J. Müller, and S. Ihlenfeldt

Inline Measurement of Process Forces and Development of a Friction Model in Abrasive Flow Machining	334
S. Roßkamp and E. Uhlmann	
Fast Evaluation of Volumetric Motion Accuracy of Multi-axis Kinematics Using a Double Ballbar	345
R. Zhou, B. Kauschinger, C. Friedrich, and S. Ihlenfeldt	
Additive Processes	
Evaluating the Cumulative Energy Demand of Additive Manufacturing Using Direct Energy Deposition	357
S. Ehmsen, L. Yi, and J. C. Aurich	
Building Blocks for Digitally Integrated Process Chains in PBF-Based Additive Manufacturing	368
M. Sjarov, N. Ceriani, T. Lechler, and J. Franke	
Correlation of Spatter Quantity and Speed to Process Conditions in Laser Powder Bed Fusion of Metals	378
E. Eschner, K. Schwarzkopf, T. Staudt, and M. Schmidt	
Investigation on Structural Integration of Strain Gauges using Laser-Based Powder-Bed-Fusion (LPBF)	387
M. Link, M. Weigold, J. Probst, R. Chadda, C. Hartmann, M. Hessinger, M. Kupnik, and E. Abele	
3D Printing Technology for Low Cost Manufacturing of Hybrid Prototypes from Multi Material Composites	396
L. Penter, J. Maier, B. Kauschinger, T. Lebelt, N. Modler, and S. Ihlenfeldt	
Automated Assembly and Robotics	
Value Stream Kinematics	409
E. Mühlbeier, P. Gönzheimer, L. Hausmann, and J. Fleischer	
Simulation-Based Robot Placement Using a Data Farming Approach . . .	419
T. Lechler, G. Krem, M. Metzner, M. Sjarov, and J. Franke	
Frequency-Based Identification of the Inertial Parameters of an Industrial Robot	429
L. Gründel, C. Reiners, L. Lienenlücke, S. Storms, C. Brecher, and D. Bitterolf	
Increasing Efficiency in Maintenance Processes Through Modular Service Bundles	439
J. Fuchs, H. Herrmann, S. J. Oks, M. Sjarov, and J. Franke	
Domain-Specific Language for Sensors in the Internet of Production . . .	448
M. Bodenbenner, M. P. Sanders, B. Montavon, and R. H. Schmitt	

An Economic Solution for Localization of Autonomous Tow Trucks in a Mixed Indoor and Outdoor Environment Using a Node Based Approach 457
 M. Zwingel, M. Herbert, M. Lieret, P. Schuderer, and J. Franke

Automated Assembly of Thermoplastic Fuselage Structures for Future Aircrafts. 467
 S. Kothe, B. Diehl, D. Niermann, L. Chen, M. Wolf, and W. Hintze

Towards Adaptive System Behavior and Learning Processes for Active Exoskeletons. 476
 B. Otten, N. Hoffmann, and R. Weidner

Machine Learning

Research on Preprocessing Methods for Time Series Classification Using Machine Learning Models in the Domain of Radial-Axial Ring Rolling 487
 S. Fahle, A. Kneißler, T. Glaser, and B. Kuhlenkötter

Process Monitoring Using Machine Learning for Semi-Automatic Drilling of Rivet Holes in the Aerospace Industry 497
 L. Köttner, J. Mehnen, D. Romanenko, S. Bender, and W. Hintze

Sustainable Interaction of Human and Artificial Intelligence in Cyber Production Management Systems 508
 P. Burggräf, J. Wagner, and T. M. Saßmannshausen

Autoconfiguration of a Vibration-Based Anomaly Detection System with Sparse a-priori Knowledge Using Autoencoder Networks 518
 J. Hillenbrand and J. Fleischer

Combining Process Mining and Machine Learning for Lead Time Prediction in High Variance Processes 528
 M. Welsing, J. Maetschke, K. Thomas, A. Gützlaff, G. Schuh, and S. Meusert

Development of a Temperature Strategy for Motor Spindles with Synchronous Reluctance Drive Using Multiple Linear Regression and Neural Network 538
 M. Weber, F. He, M. Weigold, and E. Abele

Concept for Predicting Vibrations in Machine Tools Using Machine Learning 549
 D. Barton and J. Fleischer

Automated Profiling of Energy Data in Manufacturing 559
 C. Kaymakci and A. Sauer

Automated Identification of Parameters in Control Systems of Machine Tools 568
P. Gönzheimer, A. Puchta, and J. Fleischer

Management Sciences

Process Cost Calculation Using Process Data Mining 581
A. Menges, C. Dölle, M. Riesener, and G. Schuh

Refining Circulation Factories: Classification Scheme and Supporting Product and Factory Features for Closed-Loop Production Integration 591
J. Rickert, S. Blömeke, M. Mennenga, F. Cerdas, S. Thiede, and C. Herrmann

Complexity-Oriented Description of Cyber-Physical Systems 602
A. Keuper, C. Dölle, M. Riesener, and G. Schuh

Adapted Process Model for Manufacturing Within Production Networks 611
M. Reimche, S. Berghof, and J. P. Bergmann

Organizational Agility in Development Networks 621
M. Kuhn, C. Dölle, M. Riesener, and G. Schuh

Towards a Concept for an Employee-Specific Retention Strategy in Value-Adding Areas 631
S. Korder and G. Reinhart

Identification of Project-Related Context Factors for the Tailored Design of Hybrid Development Processes 640
J. Ays, C. Dölle, M. Riesener, and G. Schuh

Systematization of Adaptation Needs in the Design of Global Production Networks 650
N. Rodemann, M. Niederau, K. Thomas, A. Gützlaff, and G. Schuh

Data-Assisted Value Stream Method 660
C. Urnauer, V. Gräff, C. Tauchert, and J. Metternich

Definition of Process Performance Indicators for the Application of Process Mining in End-to-End Order Processing Processes 670
S. Schmitz, F. Renneberg, S. Cremer, A. Gützlaff, and G. Schuh

Highly Iterative Planning of Mixed-Model Assembly Lines 680
J. Maetschke, B. Fränken, F. Saueremann, A. Gützlaff, and G. Schuh

Token-Based Blockchain Solutions for Supply Chain Strategies 689
F. Dietrich, A. Turgut, D. Palm, and L. Louw

**Determination of a Dedicated, Cost-Effective Agility
in Manufacturing Networks** 699
J. Ays, A. Gützlaff, K. Thomas, F. Berbecker, and G. Schuh

**Requirements for an Event-Based Visualization
of Product Complexity** 707
J. Koch, C. Dölle, M. Riesener, and G. Schuh

**Design of Tailored Subscription Business Models – A Guide
for Machinery and Equipment Manufacturers** 717
Y. Liu, A. Gützlaff, S. Cremer, T. Grbev, and G. Schuh

Author Index 729

Forming Machine Tools and Manufacturing Processes

Experimental Characterisation of Tool Hardness Evolution Under Consideration of Process Relevant Cyclic Thermal and Mechanical Loading During Industrial Forging	3
Modelling of Hybrid Parts Made of Ti-6Al-4V Sheets and Additive Manufactured Structures	13
Investigation of a Superimposed Oscillation Compression Process for the Production of a Bulk Component	23
Towards an Adaptive Production Chain for Sustainable Sheet-Metal Blanked Components	34
Investigation on Noise Reduction During Cutting of High-Strength Materials Based on Machine Acoustic Simulation	45
Equal-Channel-Angular-Swaging for the Production of Medical Implants Made of Fine-Grained Titanium	56
Numerical Development of a Tooling System for the Co-extrusion of Asymmetric Compound Profiles on a Laboratory Scale	66
Investigation of the Phase Transformation in Hot Stamping Processes with Regard to the Testing Facility	76
Simulation of an Electromagnetic Foil-Feeding Device	86
Extension of Process Limits with Bidirectional Deep Drawing	96
Further Development of a Hydraulically Operated Oscillation Device for Application to an Industrial Forming Process	105
Investigation of Clinched Joints – A Finite Element Simulation of a Non-destructive Approach	116
Experimental Process Design for Reclamation of Geared Components	125
A New Approach for the Evaluation of Component and Joint Loads Based on Load Path Analysis	134
Microstructure and Mechanical Properties of Thermomechanically Forged Tempering Steel 42CrMo4	142

Dynamic Performance of Polymer-Steel-Hybrids Manufactured by Means
of Process Integration 151

Investigation of the Scaling of Friction Coefficients from the Nano to the Micro
Level for Base Materials and Coatings 161

Investigation of Parameters Influencing the Producibility of Anodes
for Sodium-Ion Battery Cells 171

Numerical Investigation of an Extruded Shaft for High Temperature Applications
Manufactured by Tailored Forming 182

Introduction of Composite Hot Extrusion with Tubular Reinforcements
for Subsequent Cold Forging 193

Experimental Springback Validation of a Finite Element Model of Multi-stage
Stator Bending 202



Experimental Characterisation of Tool Hardness Evolution Under Consideration of Process Relevant Cyclic Thermal and Mechanical Loading During Industrial Forging

F. Müller^(✉), I. Malik, H. Wester, and B.-A. Behrens

Institute of Forming Technology and Machines, An der Universität 2, 30823
Garbsen, Germany
f.mueller@ifum.uni-hannover.de

Abstract. The near-surface layer of forging tools is repeatedly exposed to high thermal and mechanical loading during industrial use. For the assessment of wear resistance of tool steels, in previous work thermal cyclic loading tests were carried out to investigate changes in hardness. However, actual results of time-temperature-austenitisation (TTA) tests with mechanical stress superposition demonstrated a distinct reduction of the austenitisation start temperature indicating a change in the occurrence of tempering and martensitic re-hardening effects during forging. Therefore, the superposition of a mechanical compression stress to the thermal cyclic loading experiments is of high interest. Tests are carried out in this study to analyse hardness evolution of the tool steel H11 (1.2343) under consideration of forging process conditions. The results show that the application of compression stresses on the specimen during the temperature cycles is able to restrict tempering effects while increasing the amount of martensitic re-hardening.

Keywords: Forging · Tool hardness · Phase transformation · Wear estimation · Martensitic re-hardening · Tempering

1 Introduction

High workpiece temperatures of up to 1250 °C during forging steel result in excessive heating of the surface layer of the forging tools [1]. Numerous investigations show that high surface temperatures in combination with strong cooling due to spray cooling lead to a structural change in the tool surface layer [2]. By this means, micro-structural changes are caused leading to tool hardness changes depending mainly on the tool alloy, the maximum tool temperature and the cooling conditions [3] increasing the risk of tool failure or tool deformations [4]. However, recent studies have also proven, that mechanical stress strongly influences the austenitisation-behaviour of

hot work steels enabling the occurrence of martensitic re-hardening [5]. In general, hardness-changes have a decisive influence on the wear behaviour and thus on the tool life [6]. In each forging cycle the tools are exposed to a combination of thermal and mechanical stresses [7]. Statistical investigations on forging dies show that the main cause of failure of forging tools is due to approx. 70% abrasive wear and approx. 25% mechanical cracking [8]. In industrial practice, the type of damage is strongly dependent on the existing stress collectives. For example, increased wear appears due to thermally induced micro-cracks and abrasion in the tool surface [9]. The growth of tool wear also leads to geometric deviations and a reduction in component quality, which contradicts the demand for near-net-shape production and consistent product quality. In case of a significant wear progress or a tool breakage, high setup costs are incurred in addition to the costly production of new tools. Therefore, reliable information about the expected tool life is necessary for economical process control and the scheduling of set-up times. Moreover, for the design of wear-optimised tools a realistic prediction of the expected tool wear as a function of the forging cycles is required. In addition to the work of Klassen et al. [5], time-temperature-austenitisation (TTA) tests with mechanical stress superposition were carried out by Behrens et al. [10]. By varying the compression load between 30% and 80% of the elastic limit k_{f0} determined at 900 °C of hardened H11 tool steel, a distinct reduction of the Ac_1 temperature of approx. 40 °C was detected as shown in Fig. 1-A for every heating rate tested. The Ac_1 temperature of a tool steel is of high interest for its wear behaviour because at this temperature the phase transformation to austenite starts, which is retransformed to even harder martensite during the tool cooling [11]. In the context of this study, this effect is referred to as (martensitic) re-hardening. An exemplary application of the data from Behrens et al. [10] via an UPSTNO subroutine in the finite element software Simufact.forming 16 is presented in Fig. 1-B, indicating the area of a forging tool where the Ac_1 temperature is exceeded during the forging process. Including the consideration of mechanical stress on the Ac_1 temperature, the area, where martensitic re-hardening effects are expected ($T_{\text{process}} > Ac_1$), is significantly increased resulting in a different expected wear behaviour.

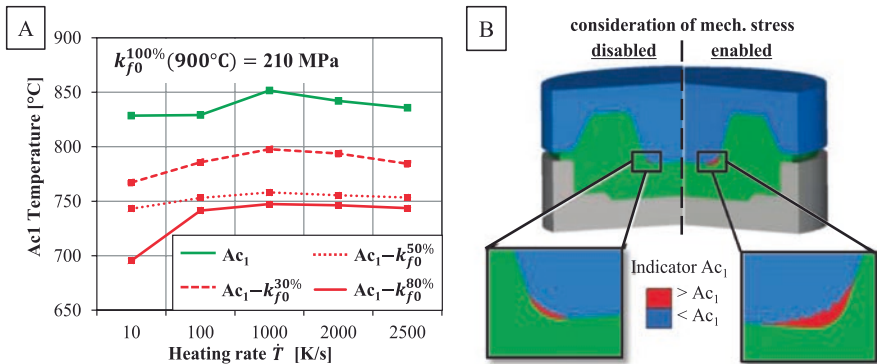


Fig. 1. Results of TTA tests with mechanical stress superposition on H11 tool steel [10] (A)/ Exemplary influence on the size of the of the martensitic re-hardening zone (red) with and without consideration of mechanical stress (B)

As a consequence, further tests are carried out in this study presenting the results of a cyclic thermo-mechanical loading to H11 tool steel. Peak temperatures are varied in regard to Ac_1 and mechanical loading in regard to the elastic limit of the material to test the influence of the parameters on tempering effects and martensitic re-hardening.

2 Methodology

For carrying out cyclic loading tests a forming dilatometer DIL805D by TA Instruments is used equipped with SiO_2 deformation punches (Fig. 2-A). Since investigations on wear-related topics are fundamentally about saving costs, the necessary testing procedure is also strongly connected to an evaluation of testing costs. Therefore, hollow samples are of high interest in order to not only to be able to achieve process relevant heating and cooling rates but also to minimise the amount of nitrogen cooling gas. This sample type is characterised by an increased specimen surface in comparison to the conventional specimen made of bulk material. Because of this decision, two main circumstances using the DIL805D had to be addressed:

1. The primary use case of the deformation unit for the DIL805 is the evaluation of mechanical properties using cylindrical bulk samples ($\varnothing 5\text{ mm} \times 10\text{ mm}$). The default hydraulic force control parameters are therefore optimised for this sample type. Using hollow samples with these parameters results in high force deviations as shown in Fig. 2-B, especially during fast heating or quenching segments, where the sample length is rapidly changing. As a consequence the controller sensitivity has to be significantly increased by reducing the proportional value to $x_p=0.007$. This system value is the most influential parameter for the determination of the control strength in proportional relation to the systems inherent control power after a control deviation is measured. In this case, less power of the hydraulic pressure pump for the regulation of the punch force has to be engaged to accommodate for the reduced specimen cross section. This change reduces force deviations during fast temperature changes to less than 10% of the specified value while allowing heating rates of up to 600 K/s.

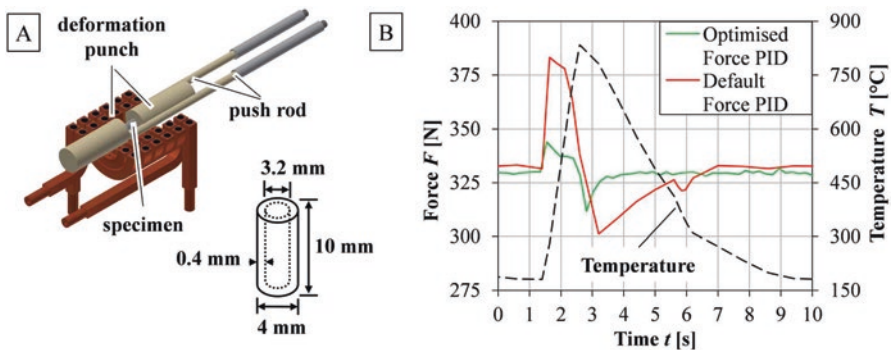


Fig. 2. Dilatometer DIL805D test apparatus and hollow specimen geometry (A)/Optimisation of force PID control parameters for hollow samples (B)

2. The DIL805D default programming capabilities are limited to a certain amount of test segments. Therefore, the DIL control software was extended by TA Instruments with a custom cycle generator module enabling the application of continuous thermal cycles with a constant mechanical stress superposition.

With this test-setup prepared, two types of tests were carried out in regard to the respective test matrices presented in Tables 1 and 2. At first, an extended cyclic re-hardening test is performed by applying sets of 25 thermo-mechanical load cycles with peak temperatures from 800 °C to 900 °C. Mechanical stress is superimposed with three levels in regard to the elastic limit k_{f0} of H11 tool steel determined at 900 °C. The aim of the test is to identify the lowest peak temperature where re-hardening effects can be observed by an increase in hardness. Also, this test is also used to investigate the relationship between the austenitisation behaviour characterised by TTA tests and the wear-relevant hardness. While the dilatometric TTA test used by Behrens et al. [10] is based on tactile measurements to identify phase transformation on a micrometre scale, the hardness evaluation features an optical measurement of indents for the determination of the hardness value. Therefore it must be assumed, that the detection resolution with this procedure is reduced, leading to the assumption that the measurable minimum temperature at which re-hardening occurs is higher compared to the TTA tests.

Table 1. Test matrix for the re-hardening study

Stress superposition [% k_{f0}]	Temperature range [°C]	Temperature Increment [°C]	Cycles	Repetitions
0	800–900	20	25	3
30				
50				
80				

Afterwards, thermo-mechanical loading tests with high cycle counts up to 2000 are carried out to estimate the effects during industrial use. Regarding peak temperatures 600 °C, 750 °C and 900 °C are used to ensure the formation of re-hardening as well as tempering effects. The thermal cycle profile using a heating rate of 500 K/s and the application of the mechanical stress superposition is identical in both parts of this study. Keeping a thermal cycle time of about eight seconds in mind, the repetition number had to be reduced to two because of the high testing time of over two hours per 1000 cycles.

Table 2. Test matrix for the high cycle loading tests

Peak temperatures [°C]	Stress superposition [% k_{f0}]	Investigated cycle numbers	Repetitions
600	0, 30, 50, 80	1, 10, 50, 100, 500, 1000, 2000	2
750			
900			

All tested samples are metallographically prepared for micro-hardness measurement at nine measuring points across the sample length as shown in Fig. 3-A. For this purpose, the samples are first cast in epoxy resin and subsequently wet grinded in several steps with SiC grinding paper ranging from a 220 to a 1200 grid. Afterwards the samples are polished three times using diamond suspension with an abrasive grain diameter of 6, 3 and 1 μm . Both operations are carried out on a Tegramin-30 sample preparation device by Struers. The embedded specimens are then etched with 5% nital acid for light microscopical images of the microstructure. For the micro-hardness measurement the standardised measuring method according to Vickers with a test load of 1.961 N (corresponds to HV0.2) is used.

3 Results and Discussion

3.1 Pretesting

In Fig. 3-B an exemplary overview of the microstructure after 10 loading cycles at 900 $^{\circ}\text{C}$ with 80% k_{f0} is presented showing a characteristic transition from the outer area of the specimen to the center. Because of heat transfer between the sample and the deformation punch leading to lower peak temperatures, the outer area is dominated by tempered ferrite with remaining martensite plates featuring a reduced hardness of 380 HV. The centre of the specimen, where the testing temperature is ensured, only consists of a fine-grained structure, which can be referred to as re-hardened martensite. Hardness in this area is significantly increased to 650 HV compared to the base hardness of 450 HV.

In this study hardness was only evaluated in the middle area of the specimen close to the central welding location of the thermocouple placed at evaluation point 5. This is achieved by statistically averaging the hardness values of the measuring points from position 4 to 6 while also calculating the standard deviation in this area to assess possible fluctuations in hardness.

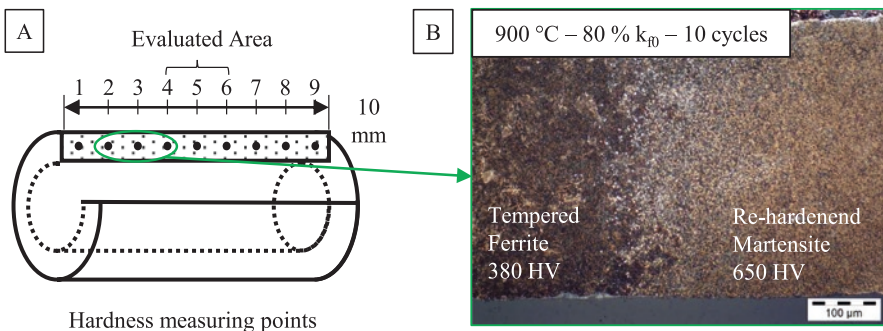


Fig. 3. Hardness measuring locations (A) and microstructural image of the transition area representing the hardness measuring locations from 2 to 4 showing tempered ferrite and re-hardened martensite after thermo-mechanical loading (B)

3.2 Re-hardening Study

As assumed in Sect. 2, the results of the re-hardening study, plotted in Fig. 4, does not show a clear conformity to the measured A_{c1} temperatures via TTA testing. While without stress superposition (0% k_{f0}) re-hardening can initially be observed at temperatures over 880 °C, the superposition with 80% of the elastic limit k_{f0} will activate this effect already at temperatures of about 850 °C. In agreement with the results of Fig. 1-A the magnitude of the impact due to the mechanical stress level decreases with increased loading. While the measured data agrees with the finding that higher mechanical load leads to lower re-hardening start temperatures in theory, the difference between all results of the mechanical stress superposition tests are relatively minor in practice. The calculated standard deviation of ± 15 HV are explained with the inherent measurement inaccuracy of the optical Vickers method. An exception is found in the hardness values of the 50% stress superposition series where the standard deviation values are significantly increased (approx. ± 45 HV). The reason for this was found in the evaluation area defined in Fig. 3-A. While in the other test series at this zone either re-hardened or tempered microstructure was found exclusively, in the prominent test series a transitional microstructure comparable to Fig. 3-B was found. A possible explanation for this are slight offsets on the thermocouple welding location or a slight non-concentric placement of the sample in regard to the deformation punches of the dilatometer leading to deviations of the temperature field applied. Keeping this in mind, it must be concluded that the superposition with mechanical stress levels over 30% of k_{f0} leads to no distinct difference on the occurrence of re-hardening effects compared to each other.

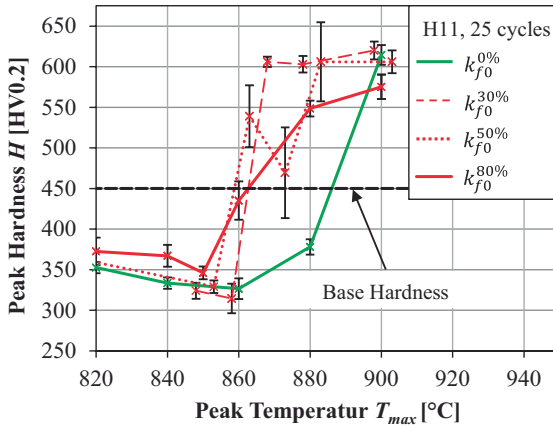


Fig. 4. Hardness over peak temperature for H11 after 25 thermo-mechanical loading cycles, heating rate: 500 K/s

3.3 High Cycle Loading

Because of the findings of the re-hardening study, only the results with mechanical loading of 80% k_{f0} and without additional loading are shown in Fig. 5 for the evaluation of the thermo-mechanical loading test at higher cycle counts and for better comprehension. In general, the results of measurements at 30% and 50% k_{f0} , which are not shown in this picture, are nearly identical to the results depicted below for 80% k_{f0} .

Regarding the three tested peak temperatures, three individual findings can be identified: After the loading at a peak temperature of 600 °C no measurable change in hardness could be observed under consideration of a minor standard deviation of less than 5 HV both with mechanical stress superposition and without. This finding indicates that the superposition applied has no influence on the material specific activation temperature for the occurrence of tempering effects.

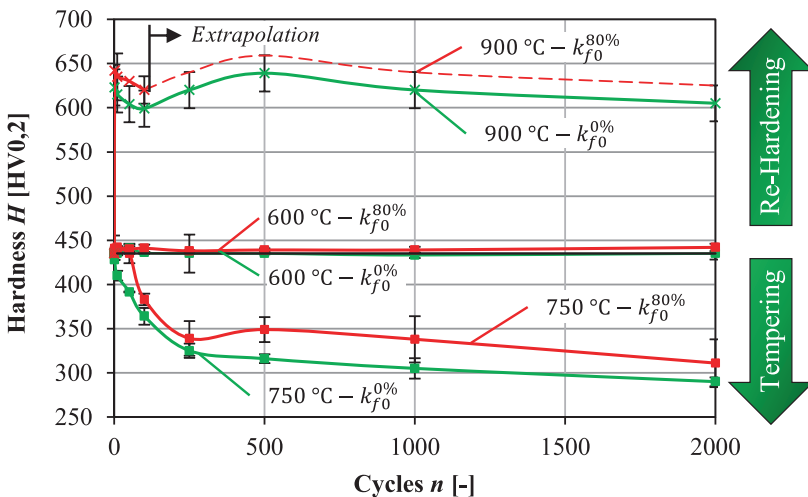


Fig. 5. Hardness results of the thermo-mechanical loading tests on H11 with cycle counts on a process relevant scale

At a peak temperature of 750 °C and up to 250 testing cycles no significant differences between all mechanical loading scenarios can be observed either. During all tests the hardness is reduced from 450 HV down to about 340 HV indicating tempering effects. However, after 500 cycles the reduction of hardness is slowed down by the application of mechanical stress superposition leading to a remaining hardness delta of approximately 30 HV over the full testing cycle spectrum. This finding is mainly explained by the diffusion properties of forcefully resolved carbon in the ordered martensitic matrix. At first, because of the high concentration gradient between matrix and microstructure, carbon can be transferred regardless of the overlaying mechanical stress leading to the identical drop in hardness. However, after the concentration compensation reached a critical point, the superposition with mechanical stress leads

to additional restraint on the martensitic structure slowing down the ongoing diffusion process. The standard deviation of the hardness values for this test series were also found to be in an acceptable range of less than ± 10 HV indicating a homogenous microstructural distribution over the evaluation area of all related samples.

At a peak temperature of 900 °C, an immediate increase of the base hardness from 450 HV to over 600 HV is measured after all loading scenarios. During all tests at 900 °C with mechanical stress superposition a steady decrease of specimen length (about 4 μm per cycle) was also observed leading to severe deformation as shown in Fig. 6-A. To prevent a collapse of the specimen, which was found to be happen after a length decrease of about 500 μm , all tests with mechanical stress superposition had to be stopped after 100 loading cycles. Since the microstructure in the deformed area presented in Fig. 6-B is dominated by re-hardened martensite, as can be derived from Fig. 3-B, transformation-induced plasticity is determined as the reason for the sample deformation. This effect describes the occurrence of plastic deformations as a result of elastic mechanical stress during a phase transformation of the microstructure from austenite to martensite [12]. In the case of this study the transformation from martensite to the smaller austenitic structure during heating leads to a reduction of the sample length which is amplified by the mechanical load. During cooling the size increase in length direction due to the retransformation to martensite is also blocked by the deformation punches. Both effects combined cause an incremental reduction of the specimen length during each loading cycle. Still, up to a cycle count of 100, the measured hardness values were approx. 30 HV higher than the measurements with no external mechanical stress applied. However, because of the slightly increased standard deviation of both testing series of about ± 15 HV, the influence of the superposed mech. loading is found to be minor in regard to the absolute achievable peak hardness. Nevertheless, the results of the test series with superposed mech. stress were extrapolated in accordance to the unloaded test results by adding a constant offset value of 30 HV to obtain a full data set for upcoming numerical material modelling.

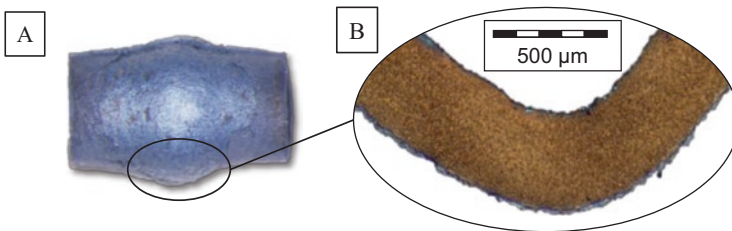


Fig. 6. Deformed specimen after 50 thermo-mechanical loading cycles at 900°C and 80% k_{10} superposition (A) with martensitic microstructure formed by re-hardening (B)

4 Summary and Outlook

In the present study, the influence of mechanical stress superposition applied to thermal-cyclic experiments to reproduce the tool load in the surface layer while forging was investigated. In previous work, the decrease of the material characteristic A_{c1}

temperature was already confirmed by dilatometric TTA tests. Now the occurrence of the associated martensitic re-hardening effects at reduced temperatures could be shown at the example of H11 tool steel. Regarding the two test series carried out in this study two main findings could be identified:

- While the TTA tests indicated a clearly measurable influence of the mech. stress level on the reduction of A_{c1} , the results of the re-hardening study were only dependent on the amount of mech. stress to a lesser degree. In summary, it was found that as long as any mechanical load was applied, a significant reduction of about 20 °C to the minimum temperature necessary for re-hardening was observed.
- As a result of the high cycle loading tests, it was shown that tempering effects are influenced by an external mech. stress superposition, resulting in slower reduction in hardness. However, the maximum amount of hardness achievable due to re-hardening was found to be only marginally influenced by the application of mech. stress superposition.

These observations indicate for future work that for more precise wear estimations based on calculated process variables, the normal mechanical contact stress on the surface layer must also be taken into account. In the next step, a user subroutine for Simufact.forming 16 will be created to visualise the material data gathered in this study. Also, widely used nitride tool layers for additional wear resistance are in the focus of upcoming investigations. Since these layers represent a significant chemical modification of the surface layer, the austenitisation and the behaviour of the hardness evolution under thermo-mechanical load will be tested analogously to this study. Finally, laboratory forging tests are planned to validate the results of the material characterization and simulations.

Acknowledgements. The authors gratefully acknowledge the support of the German Research Foundation (Deutsche Forschungsgemeinschaft - DFG) and the German Federation of Industrial Research Associations (AiF) within the projects DFG 397768783 and AiF 19647 for this research work.

References

1. Jeong, D.J., Kim, D.J., Kim, J.H., Kim, B.M., Dean, T.A.: Effects of surface treatments and lubricants for warm forging die life. *J. Mater. Process. Technol.* **113**, 544–550 (2001)
2. Yu, Z., Kuznetsov, K., Mozgova, I., Böhm, V., Gretzki, T., Nürnberger, F., Schaper, M., Reimche, W.: Modeling the relationship between hardness and spray cooling parameters for pinion shafts using a neuro-fuzzy model strategy. *J. Heat Treat. Mater.* **67**(1), 39–47 (2012)
3. Caliskanoglu, D., Siller, I., Leitner, H., Jeglitsch, F., Waldhauser, W.: Thermal fatigue and softening behaviour of hot work tool steels. In: ICT Conference, Karlstad, 10.–13.09.2002, Issue 1, pp. 707–719 (2002)
4. Marumo, Y., Saiki, H., Minami, A., Sonoi, T.: Effect of the surface structure on the resistance to plastic deformation of a hot forging tool. *J. Mater. Process. Technol.* **113**(1–3), 22–27 (2001)
5. Klassen, A., Bouguecha, A., Behrens, B.-A.: Wear prediction for hot forging dies under consideration of structure modification in the surface layer. *Adv. Mater. Res.* **1018**, 341–348 (2014)

6. Kim, D.H., Lee, H.C., Kim, B.M., Kim, K.H.: Estimation of die service life against plastic deformation and wear during hot forging processes. *J. Mater. Process. Technol.* **166**, 372–380 (2005)
7. Bernhart, G., Brucelle, O.: Methodology for service life increase of hot forging tools. *J. Mater. Process. Technol.* **87**(1–3), 237–246 (1999)
8. Kannappan, A.: Wear in forging dies - A review of world experience. *Metal Form.* **36**(12), 335–343 (1969)
9. Persson, A., Hogmark, S., Bergström, J.: Temperature profiles and conditions for thermal fatigue cracking in brass die casting dies. *J. Mater. Process. Technol.* **152**, 228–236 (2004)
10. Malik, I.Y., Lorenz, U., Chugreev, A., Behrens, B.-A.: Microstructure and wear behaviour of high alloyed hot-work tool steels 1.2343 and 1.2367 under thermo-mechanical loading. In: *Materials Science and Engineering*, vol. 629 (2019)
11. Behrens, B.-A., Puppa, J., Acar, S., Gerstein, G., Nürnberger, F., Lorenz, U.: Development of an intelligent hot-working steel to increase the tool wear resistance. In: *Tooling 2019 Conference & Exhibition*, 13.05.–16.05.2019, p. 64 (2019)
12. Behrens, B.-A., Chugreev, A., Kock, C.: Macroscopic FE-Simulation of residual stresses in thermos-mechanically processed steels considering phase transformation effects. In: *XIV International Conference on Computational Plasticity, Fundamentals and Applications COMPLAS* (2019)



Modelling of Hybrid Parts Made of Ti-6Al-4V Sheets and Additive Manufactured Structures

J. Hafenecker^{1,4}(✉), T. Papke^{1,4}, F. Huber^{2,3,4}, M. Schmidt^{2,3,4}, and M. Merklein^{1,3,4}

¹ Institute of Manufacturing Technology (LFT), Friedrich-Alexander-Universität Erlangen-Nürnberg, Egerlandstraße 13, 91058 Erlangen, Germany
jan.hafenecker@fau.de

² Institute of Photonic Technologies (LPT), Friedrich-Alexander-Universität Erlangen-Nürnberg, Konrad-Zuse-Straße 3-5, 91052 Erlangen, Germany

³ Erlangen Graduate School in Advanced Optical Technologies (SAOT), Paul-Gordan-Straße 6, 91052 Erlangen, Germany

⁴ Collaborative Research Center 814 – Additive Manufacturing, Am Weichselgarten 9, 91058 Erlangen, Germany

Abstract. The current trend of mass customization pushes conventional production techniques to their limits. In the case of forming technology, limitations in terms of adaptability and flexibility emerge, while additive manufacturing lacks in the manufacturing of large, geometrically simple components. Combining both processes has potential to use the strengths of each process and thus realize time and cost efficient mass customization. As the interactions between the processes have not been fully investigated yet, in this work a distinct modelling approach in LS-DYNA is used to examine the influence of the additively manufactured elements on the formability. Namely, varying geometric properties and number of pins created with additive manufacturing are in the focus of this research. The used material is the alloy Ti-6Al-4V, which requires processing at elevated temperatures due to its low formability at room temperature. The results show a clear influence of the additively manufactured elements on the formability.

Keywords: Additive manufacturing · Forming · Titanium

1 Introduction

Mass customization describes the industrial trend to manufacture personalized products in high production volumes [1]. This trend is pushing conventional production methods to their limits [2]. One way to overcome these limits is the combination of conventional manufacturing processes with additive manufacturing (AM) [3] with its high degree of geometric freedom [4]. However, additive manufacturing shows a deficit with regard to the manufacturing time, especially for high production volumes [3]. In contrast, sheet metal forming is highly efficient in producing large quantities.

Therefore, it is ideally suited for being combined with additive manufacturing for the production of hybrid components [5]. As a result, parts can be produced with less time, costs and energy compared to an additive only process [6]. A possible area of application for hybrid components are medical implants such as hip sockets. In this field, hybrid implants offer adaptability to patient-specific customizations, but also standard geometries, which can be produced with forming technology, to reduce production time and costs [7]. Instead of inefficiently producing the whole part with laser powder bed fusion (PBF-LB), only the customizable pins are built upon the sheet metal. As a result, standardized sheets with adaptable additively manufactured structured can be used in a deep drawing process. Thus, hybrid processes grant a leading edge in terms of manufacturing times of additively manufactured parts. Additionally, hybrid parts offer the adaptability conventional forming parts are not capable of. The used material is the titanium alloy Ti-6Al-4V because of its properties such as biocompatibility and specific strength [8]. However, high strength, low Young's modulus and limited plastic strain at room temperatures reduce the formability in cold forming processes [9]. At a temperature of 400 °C and higher, less energy is necessary for dynamic recrystallization and additional slip systems are activated [10]. Thus, experiments are performed at a temperature of 400 °C. Investigations on the combination of warm bending and PBF-LB to produce hybrid parts made from Ti-6Al-4V with one additively manufactured element (AE) show the manifold interactions between the two processes [11]. The combination of these two operations is influenced by the their sequence [11] and the interactions between the AM- [12] and the forming process [5]. Purpose of this research is to investigate these interactions, namely the influence of more than one AE on the formability of the hybrid parts made from Ti-6Al-4V in LS-DYNA to gain knowledge of the interactions. Since the AEs are the adaptable component of the hybrid part, different combinations have to be investigated since a strong influence on the formability is expected. With this intention, the following parameters are varied in this study:

- the influence numbers of AEs (*Num*) with their own layouts,
- different geometries (*Geo*),
- AE-diameters (*Dia*),
- distances to the middle (*Pos*),
- fillet radii (*Rad*).

2 Experimental Setup and Procedure

2.1 Material and Modelling Approach

In this research, the hybrid parts (Fig. 1 – right) consist of the two components: sheet material and additively manufactured elements, both made of Ti-6Al-4V. The sheet has a fine grained equiaxed $\alpha + \beta$ -microstructure. The hexagonal close packed α -titanium has a limited formability at room temperature and causes anisotropic mechanical behaviour [9]. Without any heat treatment, the additively manufactured component consists of a martensitic α' -titanium. This granular structure is harder, stronger and less ductile compared to the equiaxed microstructure of the sheet

material. The results of tensile tests performed at 400 °C (Fig. 1 – left) show the differences and thus prove the need for different material models. In order to represent these different material properties in the numerical simulation, two different material models for sheet and AE are used. A second differentiation regarding the components of the hybrid part is made on basis of the element formulation. The sheet is modelled with shell elements and seven integration points across the thickness which is common for sheet metal forming simulation [13]. Solid elements are used for the additively produced pins due to their volumetric geometry. Both components are joined via common nodes (Fig. 2 – left) in a 3D-simulation. Due to symmetries, only a quarter of the hybrid part is modelled.

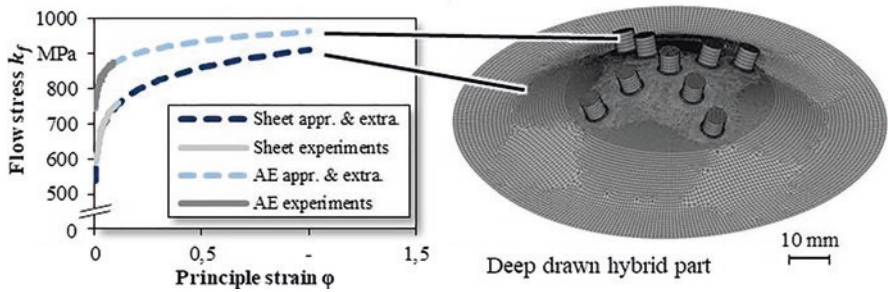


Fig. 1. Tensile flow curves of hybrid part's components at 400 °C (left); hybrid part (right)

The sheet is modelled with the LS-DYNA material model “233-CAZACU_BARLAT” that was found to represent the material behaviour precisely even at higher temperatures in [13]. This material model bases on the model of Cazacu and Barlat from 2006 [14]. However, this model is only applicable for shell elements. Thus, the material keyword “024-PIECEWISE_LINEAR_PLASTICITY”, which bases on the modelling approach of von Mises, is used for the pins. The flow curves for both material models are extrapolated using the approach of Nemat-Nasser [15]. The schematic setup of the process is shown in Fig. 2 – right.

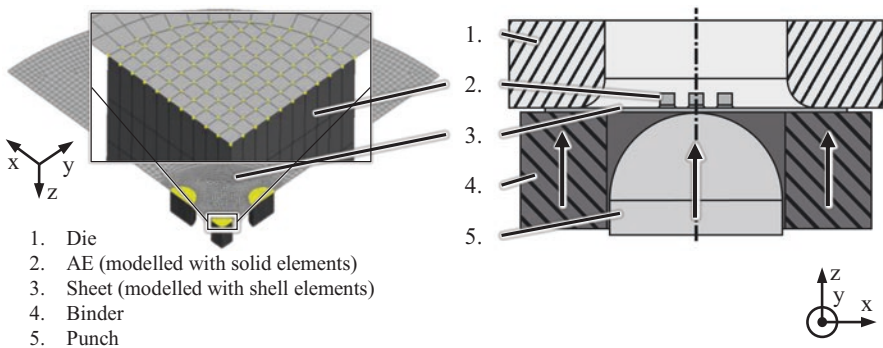


Fig. 2. Numerical representation of hybrid part with highlighted common nodes (left); schematic setup of the deep drawing process (right)

For the die, binder and punch rigid shell elements are used. The spherical punch has a diameter of 60 mm, the die clearance is 1.7 mm and the radius of the die is set to 10 mm. The sheet has a diameter of 105 mm, a thickness of 1.5 mm and the height of the pins is 5 mm. The drawing depth is set constant to 15 mm without usage of a failure criterion.

2.2 Sheet Material Modelling Validation

To assure that the process model can be used, the material model itself has to be validated first. Prior investigations used the same material model but a different sheet geometry (Fig. 3 – right), on which one AE was built after the forming process [16]. The same geometry is used for the recent material validation by thickness comparison. With this intention, the thickness distribution after the deep drawing process is calculated in the simulation and measured for real parts of a sheet without pins. The sheet thickness is measured along the x-axis in the x-z-plane. Since the numerical model only consists of a quarter of the real process, the thickness distribution is mirrored at the y-z-plane. The comparison of sheet thickness (Fig. 3) shows the high accuracy of the numerical model.

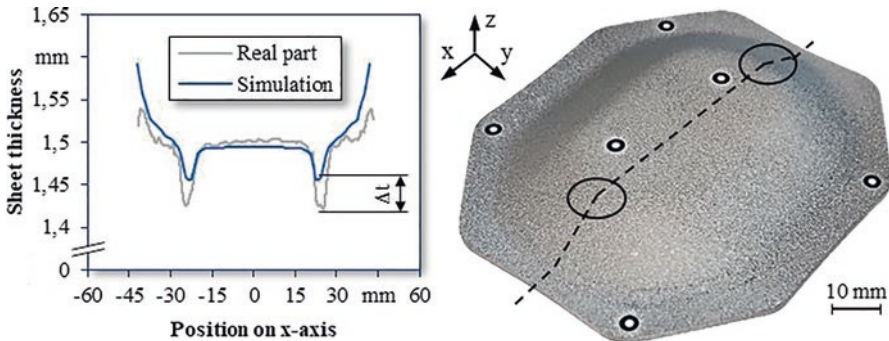


Fig. 3. Comparison of thickness distributions (left) between simulation and real part (right) along the x-axis for sheet thickness 1.5 mm; measurement path and critical spots marked (right)

Namely, maximum differences (Δt) in sheet thickness are lower than 3% of the thickness, which corresponds to 0.05 mm. Nevertheless, the critical sheet thickness reductions in the area of the punch radii are underestimated in the simulation. In particular, this is important for the spherical punch geometry where the shape is expected to lead to the highest thinning in the centre of the sheet. As this is the area where the pins are placed, the influence and resulting thickness reduction is even more critical.

2.3 Investigated Parameter Combinations

In this paper the results of the investigated influence of AE-diameter (Dia), AE-position (Pos), AE-geometry (Geo), number of additively build up pins (Num) and the size of the fillet radius at the transition (Rad) on the formability of hybrid parts